Received: 29 March 2021 | Revised: 9 December 2021 | Accepted: 11 January 2022

DOI: 10.1111/bph.15805

RESEARCH ARTICLE

Smooth muscle Rac1 contributes to pulmonary hypertension

Florian Dilasser[1] | Marc Rio[1] | Lindsay Rose[1] | Angela Tesse[1] | Christophe Guignabert[2,3] | Gervaise Loirand[1] | Vincent Sauzeau[1]

[1]Université de Nantes, CHU Nantes, CNRS, INSERM, l'institut du thorax, Nantes, France

[2]Inserm UMR_S 999 "Pulmonary Hypertension: Pathophysiology and Novel Therapies", Hôpital Marie Lannelongue, Le Plessis-Robinson, France

[3]Faculté de Médecine, Université Paris-Saclay, Le Kremlin-Bicêtre, France

Correspondence
Vincent Sauzeau, UMR Inserm 1087/CNRS 6291, IRS-UN, 8 quai Moncousu, 44007 Nantes cedex 1, France.
Email: vincent.sauzeau@univ-nantes.fr

Background and Purpose: Pulmonary hypertension (PH) is a multifactorial chronic disease characterized by an increase in pulmonary artery (PA) resistance leading to right ventricle (RV) failure. Endothelial dysfunction and alteration of NO/cGMP signalling in PA plays a major role in PH. We recently described the involvement of the Rho protein Rac1 in the control of systemic blood pressure through its involvement in NO-mediated relaxation of arterial smooth muscle cell (SMC). The aim of this study was to analyse the role of SMC Rac1 in PH.

Experimental Approach: PH is induced by exposure of control and SMC Rac1-deficient (SM-Rac1-KO) mice to chronic hypoxia (10% O_2, 4 weeks). PH is assessed by the measurement of RV systolic pressure and hypertrophy. PA reactivity is analysed by isometric tension measurements. PA remodelling is quantified by immunofluorescence in lung sections and ROS are detected using the dihydroethidium probe and electronic paramagnetic resonance analysis. Rac1 activity is determined by immunofluorescence.

Key Results: Rac1 activation in PA of hypoxic mice and patients with idiopathic PH. Hypoxia-induced rise in RV systolic pressure, RV hypertrophy and loss of endothelium-dependent relaxation were significantly decreased in SM-Rac1-KO mice compared to control mice. SMC Rac1 deletion also limited hypoxia-induced PA remodelling and ROS production in pulmonary artery smooth muscle cells (PASMCs).

Conclusion and Implications: Our results provide evidence for a protective effect of SM Rac1 deletion against hypoxic PH. Rac1 activity in PASMCs plays a causal role in PH by favouring ROS-dependent PA remodelling and endothelial dysfunction induced by chronic hypoxia.

KEYWORDS
pulmonary hypertension, Rac1, smooth muscle

1 | INTRODUCTION

Pulmonary arterial hypertension (PH) is a multifactorial and chronic disease characterized by a progressive increase in pulmonary vascular resistance and pulmonary arterial pressure that leads to right ventricle

Abbreviations: iPAH, idiopathic pulmonary arterial hypertension; LVSP, left ventricular systolic pressure; PA, pulmonary artery; PASMC, pulmonary artery smooth muscle cell; PH, pulmonary hypertension; RV, right ventricle; RVSP, right ventricular systolic pressure; SMC, smooth muscle cell.

(RV) failure and death (Simonneau et al., 2019; Thenappan et al., 2018). The increase in pulmonary vascular resistance results from both excessive vasoconstriction and vascular wall remodelling, which together lead to a narrowing of pulmonary arterial lumen. Pulmonary artery (PA) wall remodelling is a hallmark of PH and is characterized by structural changes including intimal cell proliferation, medial hypertrophy and hyperplasia, enhanced muscularity of small PA, adventitial thickening, fibrosis and complex and/or thrombotic lesions over time (Humbert et al., 2004, 2019). Current treatments such as **phosphodiesterase 5** inhibitors, **soluble guanylate cyclase** stimulators, **endothelin receptor** antagonists and activators of the **prostacyclin** pathway aim at promoting vasodilation of PA (Sitbon et al., 2019; Thenappan et al., 2018). Although these treatments improve the 6-min-walk distance, haemodynamic parameters and the quality of life of PH patients, with the exception of prostacyclin, they do not prolong survival. This suggests that targeting only vasoconstriction is not sufficient to stop disease progression (Galiè et al., 2008, 2009; McLaughlin et al., 2002, 2015; Sitbon et al., 2002, 2019).

Vascular SMCs are strongly involved in PH through their role in PA vasoconstriction but also in remodelling (Humbert et al., 2019; Lyle et al., 2017) (Thenappan et al., 2018). Small G proteins of the Rho family (**RhoA**, **Rac1** and **CDC42**) are recognized as major regulators of vascular smooth muscle cell (SMC) functions such as contraction, proliferation and migration, thus participating in the physiological regulation of blood pressure and remodelling. Accordingly, dysregulation or overactivation of Rho proteins plays a causal role in cardiovascular diseases (Loirand et al., 2013). In this way, we have shown that vascular SMC Rac1 is a regulator of systemic blood pressure through its involvement in **nitric oxide (NO)**-mediated relaxation of systemic arterial SMCs and that alteration of Rac1 signalling pathway can lead to high blood pressure (Andre et al., 2014; Sauzeau et al., 2010). Since abnormalities in **NO** production and metabolism, and NO-induced vasodilation contribute to the pathophysiology of PH (Humbert et al., 2019; Watanabe, 2018), the aim of the present study was to assess the role of Rac1 in the SMCs of PA and its involvement in PH development. Our data show that Rac1 is activated in pulmonary artery smooth muscle cell (PASMC) in a mouse model of PH induced by chronic hypoxia and in lung samples from PH patients. By using mice harbouring specific deletion of Rac1 in SMCs, we provide evidence that this activation has a causal role in the development of hypoxia-induced PH. Deletion of Rac1 in PASMCs limits hypoxia-induced PH in mice by impeding reactive oxygen species (ROS)-dependent PASMC proliferation and PA remodelling, and endothelium dysfunction.

What is already known

- Pulmonary hypertension (PH) is characterized by an increase in pulmonary artery resistance and endothelial dysfunction.
- Rac1 regulates the systemic blood pressure through its involvement in NO-mediated relaxation of smooth muscle cell.

What this study adds

- Rac1 activation is observed in pulmonary arteries of hypoxic mice and patients with idiopathic PH.
- Smooth muscle Rac1 deletion limited hypoxia-induced pulmonary artery remodelling and ROS production.

What is the clinical significance

- Our results provide evidence for a protective effect of Rac1 inhibition against hypoxic PH.

2 | METHODS

2.1 | Mice

All experimental procedures and animal care were performed in accordance with the Regional Ethical Committee for Animal Experiments of the Pays de la Loire (Authorization number 00909.01). Animal studies are reported in compliance with the ARRIVE guidelines (Percie du Sert et al., 2020) and with the recommendations made by the *British Journal of Pharmacology* (Lilley et al., 2020). Mice were housed in transparent open-top cages (29.5 × 16 × 13 cm; five mice per cage) under a 12-h light/dark cycle in a temperature-controlled and humidity-controlled room with food and water available *ad libitum*. All *in vivo* studies were carried out during the light phase of the cycle. Animal experiments were designed to have groups of equal size using randomized and blinded analysis. In some instance, however, group sizes were unequal due to unexpected loss of animals while conducting the procedures.

C57Bl/6 Rac1lox/lox (Rac1lox/lox, RRID:IMSR_NM-CKO-200212) and SMMHC-Cre (RRID:IMSR_JAX:019079) mice were crossed to produce SMMHC-Rac1lox/lox mice as previously described (Andre et al., 2014). Considering that the SMMHC-Cre construct is carried on the Y chromosome, only male mice were analysed in this study. Eight-week-old SMMHC-$Rac1^{lox/lox}$ males were treated with **tamoxifen** (intraperitoneally, 1 mg·d^{-1} in sunflower oil) for five consecutive days during 2 weeks to induce Rac1 deletion in smooth muscle cells (SM-Rac1-KO). Tamoxifen-treated $Rac1^{lox/lox}$ mice were used as control (SM-$Rac1^{lox/lox}$).

2.2 | Hypoxia-induced pulmonary hypertensive (PH) mice

To induce PH, mice were exposed to chronic hypoxia in a gaseous hypoxic chamber providing nitrogen injection to obtain 10% O_2 for

28 days (five mice per cage). Mice exposed to normoxia (21% O_2) for 28 days were used as normoxic controls (five mice per cage).

2.3 | Right and left ventricular systolic pressure (RVSP and LVSP)

As previously described (Dumas de la Roque et al., 2017), RVSP and LVSP were measured in non-ventilated mice under isoflurane anaesthesia. To maintain the body temperature, mice were maintained on a heated blanket. At the end of the experimemt, mice were killed by exsanguination. Mice were thoracotomized and a heparin-filled hypodermic needle coupled to a polyethylene catheter was inserted in subdiaphragmatic directly into the right or the left ventricle. RVSP and LVSP were measured with a fluid-filled pressure sensor connected to the PowerLab recording unit (AD Instruments, RRID:SCR_018833) and recorded with the LabChart software (AD Instruments, RRID:SCR_001620).

2.4 | Right ventricular (RV) hypertrophy measurements

After exsanguination, the right ventricle (RV) was separated from the left ventricle plus septum (LV + S). The RV/(LV + S) ratio (Fulton index) was then determined from the tissue weight.

2.5 | *Ex vivo* pulmonary artery (PA) reactivity

Murine PA were cleaned, cut in rings and mounted on a multichannel isometric myograph (Danish Myo Technology, Aarhus, Denmark) in Krebs–Henseleit physiological solution (in mol·L^{-1}: 118.4 NaCl, 4.7 KCl, 2 $CaCl_2$, 1.2 $MgSO_4$, 1.2 KH_2PO_4, 25 $NaHCO_3$, and 11 glucose) bubbled with carbogen (5% CO_2–95% O_2 at 37°C. A pretension of 10 mN was applied. The wire myograph was connected to a digital data recorder (MacLab/4e, AD Instruments, RRID:SCR_018833), and recordings were analysed using LabChart software (AD Instruments, RRID:SCR_0017551, version #7). Concentration–response curves to KCL and **endothelin-1 (ET-1)** were obtained by measuring the amplitude of the contractile responses to increasing concentration of KCl (30 mmol·L^{-1} to 110 mol·L^{-1}), ET-1 (10^{-9} mol·L^{-1} to 10^{-6} mol·L^{-1}) or **5-HT** (10^{-8} mol·L^{-1} to 10^{-4} mol·L^{-1}). Endothelium/NO-dependent and independent relaxations were tested by adding increasing concentrations of **acetylcholine (ACh**; 10^{-8} mol·L^{-1} to 10^{-4} mol·L^{-1}) or *S*-nitroso-*N*-acetyl-D,L-penicillamine (SNAP; 10^{-8} mol·L^{-1} to 10^{-4} mol·L^{-1}) to rings pre-contracted by **phenylephrine** (PhE, 1 μmol·L^{-1}) and were quantified as the percentage of the maximal PhE-induced contraction.

2.6 | Lung tissue preparation

Mice lungs were fixed in 4% paraformaldehyde (PFA) for 48 h and embedded into paraffin. These samples were then sliced in 7-μm-thick sections. For immunofluorescence analyses and ROS detection assay, mice lungs were placed into Tissue-Tek O.C.T. Compound (Sakura Finetek) and snap-frozen in liquid nitrogen before the realization of 10-μm-thick sections. Human lung biopsies were fixed in 4% PFA and embedded in paraffin. The Immuno-related procedures used comply with the recommendations made by the *British Journal of Pharmacology* (Alexander et al., 2018).

2.7 | Measurement of PA remodelling

Lung sections were stained by immunohistochemistry with anti-SM22α antibody (Abcam, RRID:AB_443021) on haematoxylin and eosin-stained sections for visualization of SMC. Sections were then observed (fluorescence microscope, Nikon) and analysed (Fiji/ImageJ software, RRID:SCR_002285 and RRID:SCR_003070). PA muscularization was then quantified as the percentage of SM22α positive distal PA (intra-alveolar vessels <100 μm) within the section. Five-μm-thick sections were analysed to calculate a mean value in each animal. The percentage of medial thickness of muscularized PA was determined as [(2 × medial wall thickness/external diameter) × 100].

2.8 | Human lung specimens

Human lung specimens were obtained during lung transplantation in patients with idiopathic pulmonary arterial hypertension (iPAH) and during lobectomy or pneumonectomy for localized lung cancer in control subjects. Preoperative echocardiological evaluation, including echocardiography, was performed in the control subjects to rule out PH, and the lung specimens from the control subjects were collected at a distance from the tumour foci. The absence of tumoral infiltration was retrospectively established in all tissue sections by the histopathological analysis. This study was approved by the local ethics committee (CPP Ile-de-France VII, Le Kremlin-Bicêtre, France). All enrolled patients gave written approval. As these biopsies are not easy to obtain and in order to maintain homogeneous groups, we included three samples in each group. Thus, no statistical analysis was performed on this study.

2.9 | Analysis of Rac1 activity

Human pulmonary biopsies and lungs paraffin-embedded sections were deparaffinized and permeabilized (PBS + 0.1% Triton-X100) before incubation with anti-Rac-GTP antibody (NewEast Biosciences, RRID:AB_1961793) (1/1000) overnight at room temperature. After three washes in PBS, sections were incubated for 1 h at room temperature with the secondary Alexa568-labelled anti-rabbit antibody (RRID:AB_10563566) (1/1000). Anti-SM22α antibody (Abcam) (1/500, overnight at room temperature) with a secondary Alexa488-labelled anti-mouse antibody (RRID:AB_138404) (1/1000,

1 h at room temperature) were used to localize smooth muscle. To quantify Rac-GTP levels within SMC, Rac-GTP fluorescence intensities were measured with Fiji (Fiji, RRID:SCR_002285) inside a mask delimited by SM22α positive cell areas and normalized to the control condition. To emphasize the specificity of Rac-GTP signal within SMC, an intensity profile was realized on Fiji along the designated line. To allow the comparison between them, each channel intensities was normalized individually as follow: - lowest intensity level = 0 A.U. and highest intensity level = 1 A.U.

2.10 | Cell culture

Pulmonary artery smooth muscle cells (PASMCs) were isolated from PA of SM-Rac1$^{lox/lox}$ mice. Tissues were cleaned manually and digested for 1 h with collagenase II (1 mg·ml^{-1}, Worthington Biochemical) at 37°C under agitation. Cells were cultured in Dulbecco modified Eagle medium (Gibco) containing 10% FBS, 1 g·L^{-1} glucose, 100 units·ml^{-1} penicillin, and 100 μg·ml^{-1} streptomycin at 37°C and 5% CO_2. All experiments were performed between passages 1 and 3.

2.11 | ROS detection assay

For tissue ROS detection, cryosection (10 μm) of unfixed snap-frozen lungs were incubated in 10-μM dihydroethidium (DHE, Invitrogen) for 30 min incubation at 37°C. Sections were then mounted with Prolong™ Gold antifade reagent containing **DAPI** (Invitrogen). For *in vitro* ROS detection, 6000 PASMCs per well were seeded into 8-well ibidi μ-Slide (IbiTreat) and allowed to adhere during 6 h and then serum starved during 24 h. When indicated, cells were pre-incubated with 10^{-5} M of EHT1864 (Tocris Bioscience) or 1.5 mmol·L^{-1} of tempol (Sigma-Aldrich) during 30 min. Cells were placed in normoxic or hypoxic (1% O_2) conditions in a Heracell 150 incubator (Kendro) during 6 h. Then cells were incubated with 10 μmol·L^{-1} at 37°C for 15 min and fixed with 4% PFA for 10 min. After fixation, cells were incubated with Hoescht to stain nuclei. Images were captured with an inverted microscope (Nikon) in epifluorescence. DAPI and Hoescht staining were detected at 405 nm, and oxidized DHE was detected at 555 nm. A threshold mask removing the background signal was applied to allow the detection of dihydroethidium positive cells.

2.12 | Superoxide ion measurement by electronic paramagnetic resonance (EPR)

Mice lungs were incubated in a Krebs–Hepes solution with 500 μM of 1-hydroxy-3methoxycarbonyl-2,2,5,5-tetramethylpyrrolidin (CMH; Noxygen), 25-μM deferoxamine (Sigma-Aldrich) and 5-μM DETC (Sigma-Aldrich) and frozen in liquid nitrogen. The samples were analysed using a table-top x-band spectrometer Miniscope (Magnettech, MS5000). The instrument settings and the modality of signal quantification were previously described (Tesse et al., 2021).

2.13 | Xanthine oxidase activity assay

Mice lungs were homogenized in 100-mM Tris-HCl, pH 7.5, containing 1× protease inhibitors (Sigma-Aldrich). Xanthine oxidase activity was measured in the lungs with a fluorometric assay kit (Cayman Chemical) according to manufacturer's instructions.

2.14 | RNA extraction and real-time PCR

Total RNA was extracted from the pulmonary arteries with TRIZOL reagent (Life Technologies) according to the manufacturer's instructions. One microgram of RNA was used for reverse transcription with High-Capacity cDNA Reverse Transcription Kit (Life Technologies). Real-time PCR using TaqMan probes was performed in 7900HT Fast Real-Time PCR System (Applied Biosystems). The expression of Hif1a (item number Mm00468869_m1, ThermoFisher), NOS3 (eNOS) (item number Mm00435217_m1, ThermoFisher), Nox1 (item number Mm00549170_m1, ThermoFisher), Cybb (Nox2) (item number Mm01287743_m1, ThermoFisher), GAPDH (item number Mm99999915_g1, ThermoFisher) and HPRT (item number Mm03024075_m1, ThermoFisher) was analysed. Natural product studies are reported in compliance with the recommendations made by the British Journal of Pharmacology (Izzo et al., 2020).

2.15 | Pulmonary artery smooth muscle cells (PASMCs) proliferation

Ten thousand PASMCs per well were seeded in 24-well plate and allowed to adhere during 6 h and then serum-starved during 24 h. When indicated, cells were pre-incubated with 10–5 mol·L^{-1} of EHT1864 (Tocris Bioscience) or 1.5 mmol·L^{-1} of tempol (Sigma-Aldrich) during 30 min. Cells were placed in normoxia or hypoxia (1% O_2) in a Heracell 150 incubator (Kendro) during 96 h, and time-lapse images were captured for 96 h (1 image/15 min) on a JuliStage microscope (NanoEntek, Seoul, Korea). The number of dividing cells during this time was then counted.

2.16 | Statistics

Data and statistical analysis complied with the recommendations of the *British Journal of Pharmacology* on experimental design and analysis (Curtis et al., 2018). Data analysis was performed in a blinded manner wherever possible. For multiple comparisons, the one-way ANOVA test was used followed by Tukey's post-test to specifically compare indicated groups. For multiple comparison of contractility studies, the two-way ANOVA test was used followed by a Bonferroni post-test. For two group comparisons, the Mann–Whitney test was performed. Post hoc tests were conducted only if F in ANOVA achieved $P < 0.05$. Sample size subjected to statistical analysis was at least five animals per group ($n = 5$, where n is the number of independent values). Data analysis was performed using the GraphPad Prism software (GraphPad Prism, RRID:SCR_002798). The threshold for statistical significance was set at $P < 0.05$.

2.17 | Materials

5-HT, ACh, phenylephrine, 1-hydroxy-3methoxycarbonyl-2,-2,5,5-tetramethylpyrrolidin (CMH) deferoxamine, DETC from Sigma Aldrich Chimie S.a.r. 80 Rue de Luzais L' Isle St. Quentin Fallavier Cedex 38297 France.

Tissue Tek from Sakura Finetek, 18 rue Hergé Parc Scientifique de la Haute Borne 59650 Villeneuve d'Ascq. SM22a antibody from Abcam, 24 rue Louis Blanc75010 PARISFRANCE. Rac-GTP antibody from NewEast Biosciences, 1150 First Avenue, Suite 501A King of Prussia, PA 19406 USA. Collagenase from Worthington, Worthington Biochemical Corporation, 730 Vassar Ave., Lakewood, NJ 08701, USA. Cell culture medium, Tirol, DHE and DAPI from Thermo Fisher, Life Technologies SAS16 Avenue du QuébecBP 30210, F – 91941 Courtaboeuf Cedex (Villebon-sur-Yvette). EHT1864 from Tocris, 19 Rue Louis Delourmel 35230 Noyal Châtillon sur SeicheFrance. CMH from Noxygen, Lindenmatte 42,79215 Elzach, Germany.

2.18 | Nomenclature of targets and ligands

Key protein targets and ligands in this article are hyperlinked to corresponding entries in the IUPHAR/BPS Guide to PHARMACOLOGY http://www.guidetopharmacology.org and are permanently archived in the Concise Guide to PHARMACOLOGY 2021/22 (Alexander, Christopoulos, et al., 2021; Alexander, Fabbro, et al., 2021).

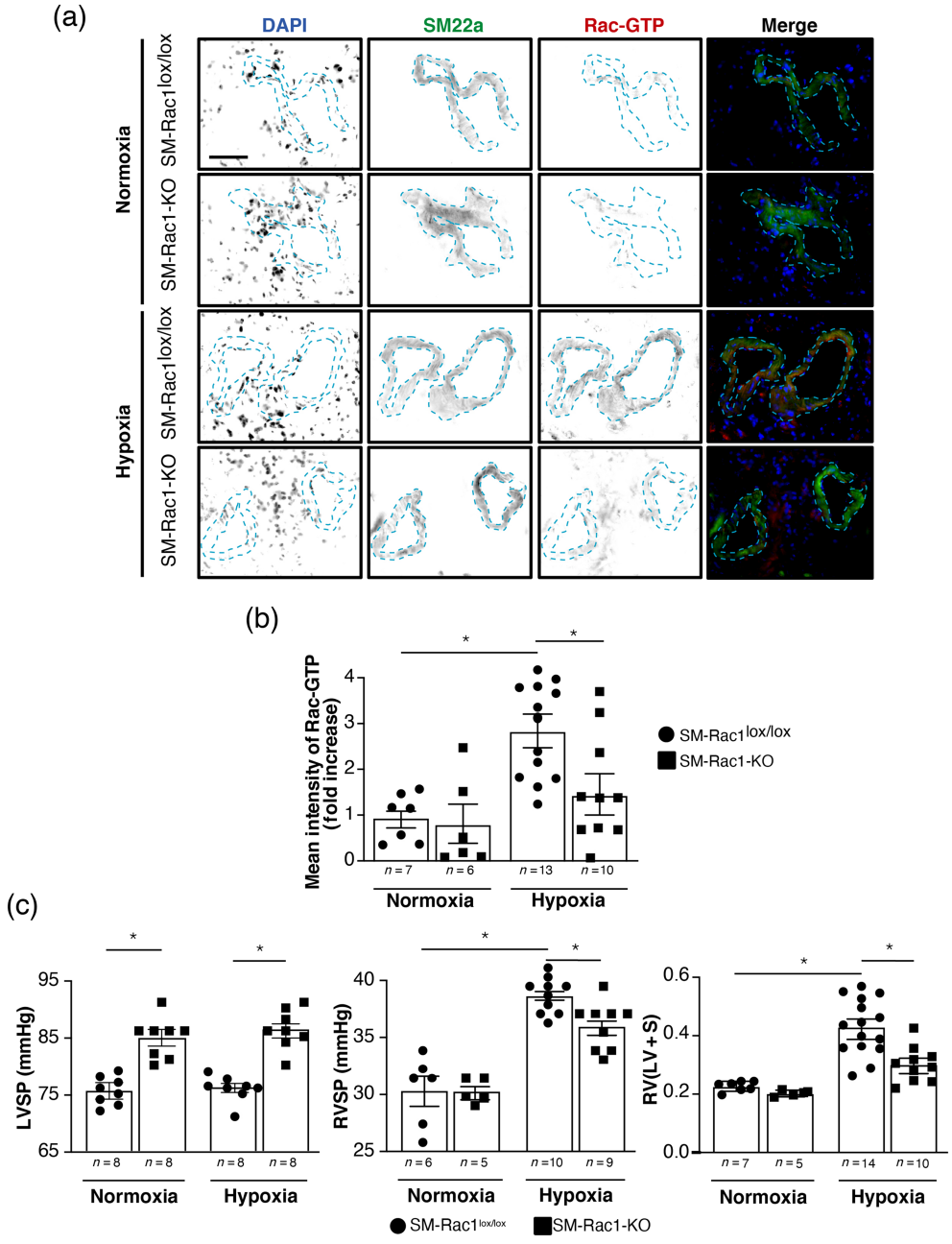

FIGURE 1 Smooth muscle (SM) Rac1 deletion prevents chronic hypoxia-induced increase in right ventricular systolic pressure and right ventricular remodelling. (a) Representative images of Rac-GTP immunofluorescence (red) in cryosections of lung from SM-Rac1$^{lox/lox}$ and SM-Rac1-KO mice exposed for 4 weeks to normoxia or hypoxia. Nuclei are detected by DAPI staining (blue) and smooth muscle by SM22α immunofluorescence labelling (green). Scale bar = 80 μm. (b) Quantification of Rac-GTP labelling fluorescence intensity in SMCs. (c) Right ventricular systolic pressure (RVSP, left panel), left ventricular systolic pressure (LVSP, middle panel) and Fulton index (RV/(LV + S); right panel) in SM-Rac1$^{lox/lox}$ and SM-Rac1-KO mice exposed for 4 weeks to normoxia or hypoxia. Data are expressed as mean ±SEM. *P < 0.05

3 | RESULTS

3.1 | Rac1 contributes to pulmonary hypertension (PH) development

We first assessed the level of Rac1 activation by immunofluorescence with a conformational sensitive anti-Rac1-GTP antibody in lung sections from normoxic and hypoxic mice. Rac1-GTP staining was significantly increased in PA walls of hypoxic SM-Rac1$^{lox/lox}$ mice compared to normoxic SM-Rac1$^{lox/lox}$ mice, while in contrast, Rac1-GTP fluorescence remained as weak as that of normoxic SM-Rac1-KO mice in hypoxic SM-Rac1-KO mice (Figure 1a,b). Rac1-GTP labelling co-localized with SM22α staining indicating that the increased Rac1 activity observed in PA of hypoxic SM-Rac1$^{lox/lox}$ mice occurred in PASMC (Figure 1a).

As expected, SM-Rac1$^{lox/lox}$ mice exposed to hypoxic condition developed PH characterized by a strong elevation of RVSP and a right ventricular remodelling attested by the increase in the Fulton index (Figure 1c). Deletion of Rac1 in SMC reduced PH as shown by the 30% decrease in RVSP and the 60% decrease in right ventricular hypertrophy in hypoxic SM-Rac1-KO mice compared to hypoxic SM-Rac1$^{lox/lox}$ mice (Figure 1c). As previously described, SM-Rac1-KO mice develop a systemic hypertension associated with an increase of LVSP (Andre et al., 2014). Under hypoxic condition, the deletion of Rac1 in SMC has no effect on LVSP. These results show that Rac1 is activated in PASMC of hypoxic mice and contributes to the pathogenesis of PH.

3.2 | SM-Rac1 deletion has no effect on the contractile properties of PA

To determine whether the involvement of Rac1 in PH was due to its role in the modulation of the vascular tone (Andre et al., 2014), we measured *ex vivo* contractile properties of PA from normoxic and hypoxic SM-Rac1$^{lox/lox}$ and SM-Rac1-KO mice. Contractile responses of PA to KCl and ET-1 were similar in SM-Rac1$^{lox/lox}$ and SM-Rac1-KO mice both in normoxic and hypoxic conditions (Figure 2). Contractile responses to 5-HT were increased in hypoxic conditions compared to normoxia but were similar in SM-Rac1$^{lox/lox}$ and SM-Rac1-KO mice (Figure 2). Regarding vasodilation,

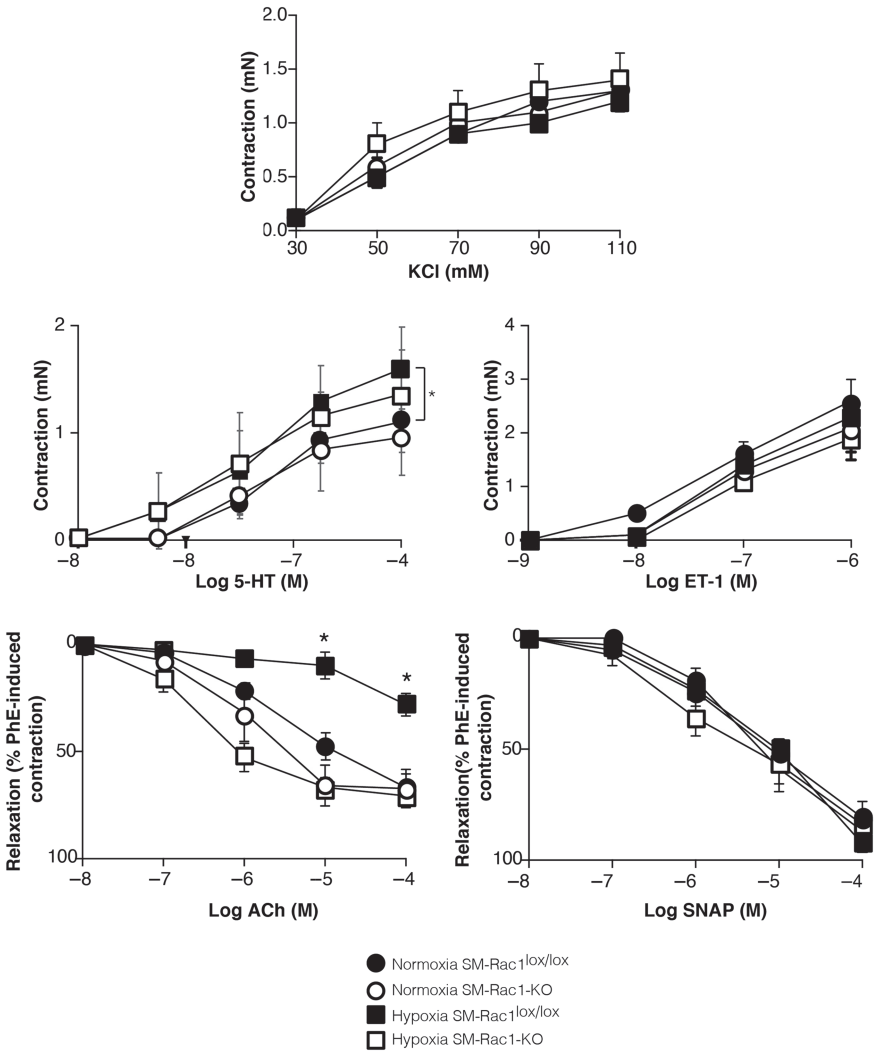

FIGURE 2 Smooth muscle Rac1 deletion prevents hypoxia-induced reduction of endothelium-dependent relaxation. Contractile responses to potassium chloride (KCl), 5-HT and endothelin-1 (ET-1), and relaxation of phenylephrine (PhE)-induced tension (1 μM) by acetylcholine (ACh) and *S*-nitroso-*N*-acetyl-D,L-penicillamine (SNAP) in pulmonary artery (PA) from SM-Rac1$^{lox/lox}$ and SM-Rac1-KO mice exposed for 4 weeks in normoxia or hypoxia (Normoxia SM-Rac1$^{Lox/Lox}$ $n = 9$ mice; Normoxia SM-Rac1-KO $n = 7$ mice; hypoxia SM-Rac1$^{Lox/Lox}$ $n = 11$ mice; hypoxia SM-Rac1-KO $n = 5$ mice). Data are expressed as mean ± SEM. *$P < 0.05$

ACh-induced NO-dependent relaxation was similar in PA from normoxic SM-Rac1$^{lox/lox}$ and SM-Rac1-KO mice, suggesting that Rac1 is not involved in NO-mediated relaxation of PASMC in basal conditions (Figure 2). Chronic exposure of SM-Rac1$^{lox/lox}$ mice to hypoxia decreased ACh-mediated relaxation of PA, attesting the endothelium dysfunction known to be associated with hypoxic PH. This defect in endothelium-derived NO-dependent relaxation is not observed in PA from hypoxic SM-Rac1-KO mice, suggesting that Rac1 in PASMC is involved in hypoxia-induced loss of NO-induced PA dilation (Figure 2). To directly assess the role of Rac1 in NO-signalling pathway in PASMC, we then used the NO donor SNAP, which directly triggers guanylate cyclase activation, cyclic GMP (cGMP) production and relaxation, independently of the endothelium (Figure 2). Concentration-relaxation response curves to SNAP were similar in PA from normoxic SM-Rac1$^{lox/lox}$ and SM-Rac1-KO mice, confirming that Rac1 is not involved in cGMP signalling-mediated relaxation of PASMC in basal conditions. Chronic exposure to hypoxia did not modify the endothelium-independent vasodilator effect of SNAP, both in SM-Rac1$^{lox/lox}$ and SM-Rac1-KO mice (Figure 2). These results indicate that Rac1 in PASMC is neither involved neither in intracellular signalling mechanisms inducing contraction nor in cGMP signalling mediating NO-dependent relaxation. However, they show that PASMC Rac1 deletion prevents hypoxia-induced defect in endothelium/NO-dependent relaxation suggesting a role of PASMC Rac1 upstream in the effect of NO on PASMC.

3.3 | Rac1 is required for hypoxia-induced PA remodelling

To assess the role of Rac1 in hypoxia-induced PA remodelling, muscularization of small PA has been analysed on lung sections by immunohistochemical labelling with an antibody that recognizes the SMC phenotypic marker SM22α. SM22α staining was weak in lung sections from normoxic SM-Rac1$^{lox/lox}$ and SM-Rac1-KO mice (Figure 3). Exposure to chronic hypoxia increased the number and the thickness of muscularized distal PA in SM-Rac1$^{lox/lox}$ mice but only had very limited effect on PA wall structure in SM-Rac1-KO mice (Figure 3). These observations suggest an essential role of SM Rac1 in PA remodelling associated with hypoxia-induced PH.

3.4 | Rac1 is essential for hypoxia-induced ROS production in the lung

Rac1 is well known for its essential role in ROS production through the regulation of **NADPH oxidase** activity (Hordijk, 2006) and ROS

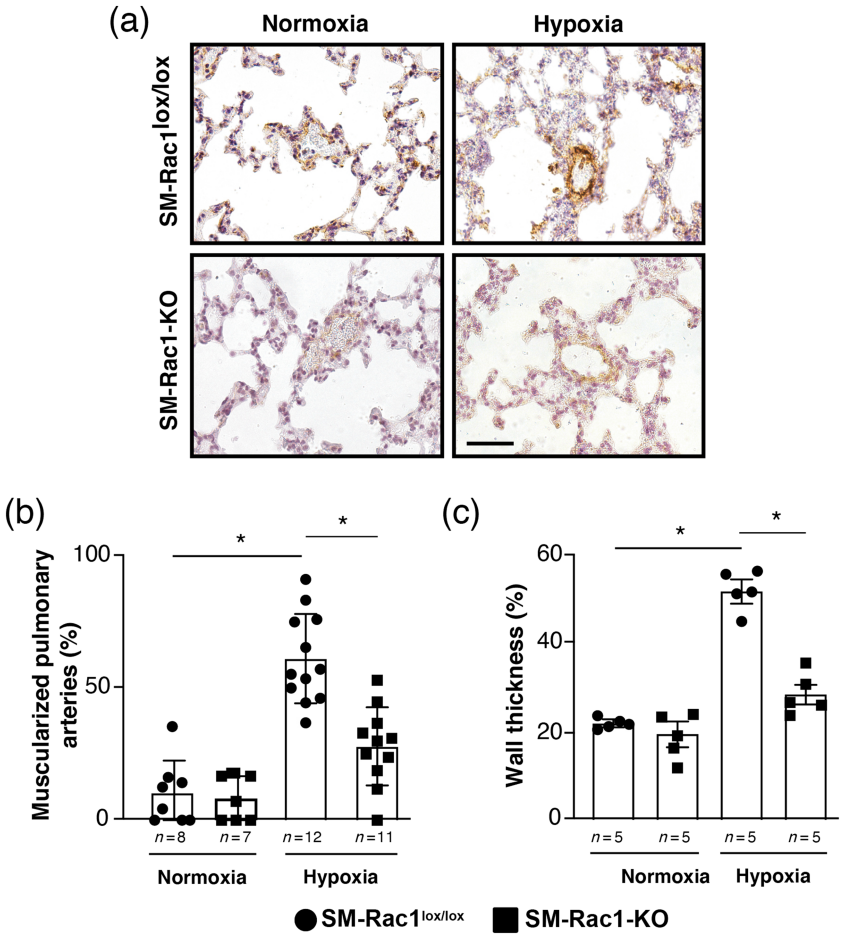

FIGURE 3 Smooth muscle Rac1 deletion prevents pulmonary artery (PA) remodelling induced by hypoxia. (a) Representative images of SM22alpha labelling on haematoxylin and eosin-stained sections of lung from SM-Rac1$^{lox/lox}$ and SM-Rac1-KO mice exposed for 4 weeks to normoxia or hypoxia. Scale bar = 80 μm. (b and c) quantification of the number of muscularized PA (b) and wall thickness (c). Data are expressed as mean ± SEM. *P < 0.05

stimulate SMC proliferation (Li et al., 2014; Wang et al., 2014; Wang & Sun, 2010). In addition, lung ROS levels are increased in chronically hypoxic mice (Fresquet et al., 2006; Liu et al., 2006). We thus hypothesize that the role of Rac1 in PA remodelling in hypoxic PH can be related to ROS production. To address this hypothesis, we measured ROS production by dihydroethidium staining in lung cryosections from normoxic and hypoxic SM-Rac1$^{lox/lox}$ and SM-Rac1-KO mice. Dihydroethidium labelling was similarly weak in both normoxic SM-Rac1$^{lox/lox}$ and SM-Rac1-KO mice indicating a low ROS production (Figure 4). The strong rise in dihydroethidium staining in hypoxic SM-Rac1$^{lox/lox}$ mice demonstrated an increase in ROS production detection in both PA and lung parenchyma (Figure 4a,b). This hypoxia-induced stimulation of ROS production was significantly reduced in PA and marginally decreased in the lung parenchyma of hypoxic SM-Rac1-KO mice (Figure 4a,b). These observations were confirmed by electronic paramagnetic resonance, demonstrating that Rac1 deletion in SMC prevents hypoxia-induced superoxide ion (O_2^-) overproduction in lungs (Figure 4c). This result is not related to a significant modification in xanthine oxidase activity (Figure 4c) or expression of major drivers of ROS production such as **NOX1**, **NOX2**, e**NOS** (NOS3) and **HIF1a** (Figure 4d). These results suggest that PASMC Rac1 plays a critical and a direct role in hypoxia-induced ROS production in the lungs.

3.5 | Rac1 is required for hypoxia induced PASMC proliferation

We next wanted to investigate the role of Rac1 in ROS production and PASMC proliferation by a pharmacological approach *in vitro*. As shown in Figure 4e, hypoxia induced increased ROS production and PASMC proliferation, both of which were suppressed by Rac1

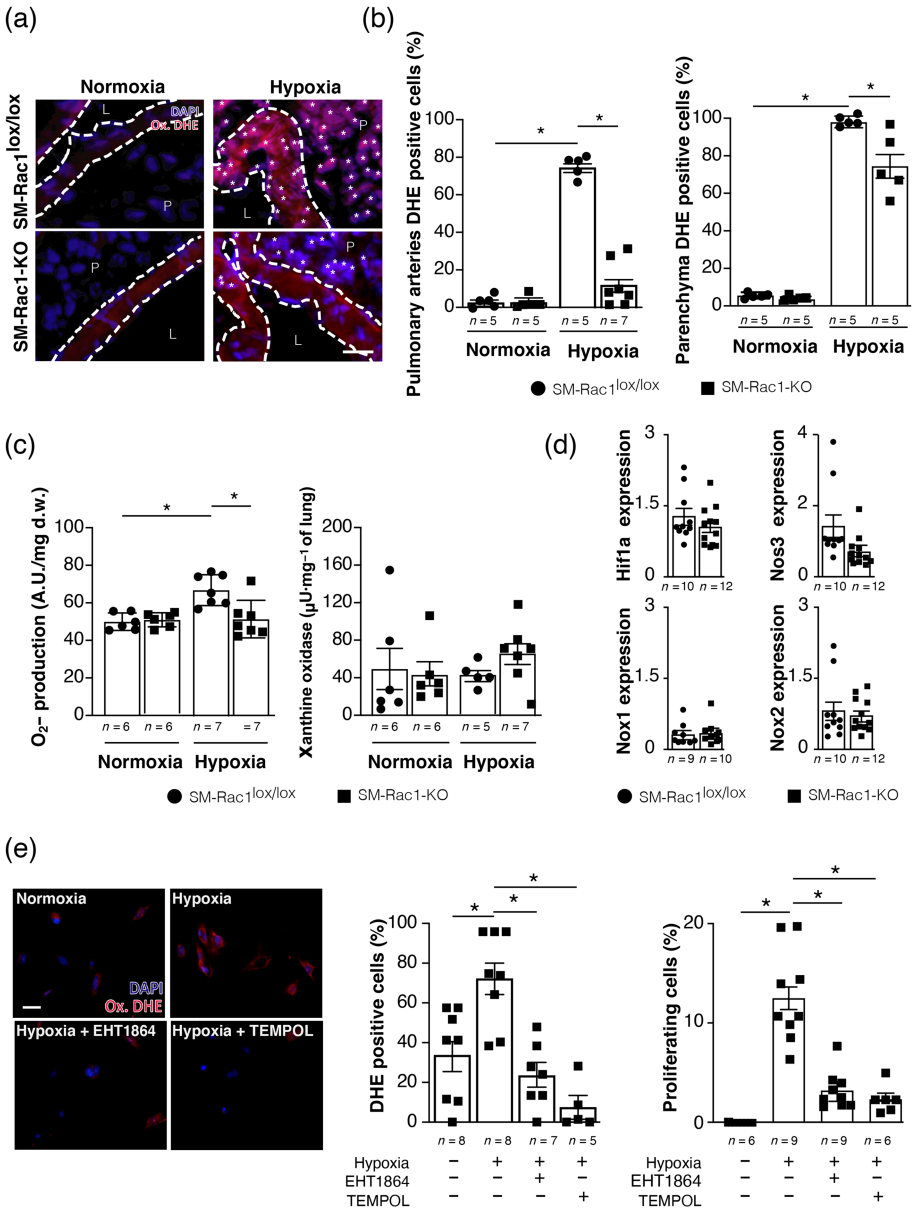

FIGURE 4 Smooth muscle Rac1 deletion prevents hypoxia-induced ROS production in pulmonary artery (PA) and pulmonary artery smooth muscle cell (PASMC) proliferation. (a) Representative images of dihydroethidium (DHE) staining of lung sections from SM-Rac1$^{lox/lox}$ and SM-Rac1-KO mice exposed for 4 weeks to normoxia or hypoxia. Scale bar = 20 μm. L, lumen; P, parenchyma; * indicates DHE positive cell. (b) Quantification of DHE positive cells in PA (left panel) and in lung parenchyma (right panel). Data are expressed as mean ± SEM. *P < 0.05. (c) Detection of O_2^- by electronic paramagnetic resonance (right panel) and xanthine oxidase activity in lungs from SM-Rac1$^{lox/lox}$ and SM-Rac1-KO mice exposed for 4 weeks to normoxia or hypoxia (left panel). Data are expressed as mean ± SEM. *P < 0.05. (d) Analysis by real-time PCR of the relative expression of HIF1a, eNOS (NOS3), NOX1 and NOX2 in pulmonary arteries from SM-Rac1$^{lox/lox}$ and SM-Rac1-KO mice exposed for 4 weeks to hypoxia compared to SM-Rac1$^{lox/lox}$ exposed for 4 weeks to normoxia. Data are expressed as mean ± SEM. (e) Representative images of DHE (red) and DAPI (blue) staining of PASMCs cultured in normoxic or hypoxic condition, and quantification of DHE positive cells and PASMCs proliferation. When indicated, cells were treated with EHT1864 (10^{-5} M) or 1.5-mM tempol. Scale bar = 10 μm. Data are expressed as mean ± SEM. *P < 0.05

inhibition of by EHT1864 or the antioxidant tempol. These results revealed that hypoxia-induced ROS production and the resulting ROS-mediated PASMC proliferation depend on Rac1.

3.6 | Rac1 is overactivated in PA of idiopathic pulmonary arterial hypertension (iPAH) patients

In order to assess whether SMC Rac1 may play a role similar to that observed in mice in the pathogenesis of PH in humans, we performed Rac1-GTP immunostaining in lungs specimens from PH patients (Figure 5). As expected, immunostaining of PASMC by the anti-SM22α antibody shows the thickening of the medial layers of the PA in explanted lungs from iPAH patients compared to control samples (Figure 5a). The weak Rac1-GTP immunostaining in control lung samples indicated a low level of active Rac1 in these subjects. In contrast, the strong fluorescence intensity of Rac1-GTP observed in iPAH patient samples showed that PH is associated with a strong Rac1 activity in the PA (Figure 5a,b). Analysis of the spatial profile of fluorescence intensities revealed that active Rac1 is specifically localized in PASMC, in agreement with our observation in the experimental model of PH in mice (Figure 5c).

4 | DISCUSSION

Our study demonstrates an increase in Rac1 activity in human and murine PASMCs during PH. The specific deletion of Rac1 in SMC limits the rise in RSVP and PA remodelling induced by chronic hypoxia, suggesting a causal role of SM Rac1 activity in the development of PH. Our results thus show that, in contrast to systemic circulation (Andre et al., 2014; Sauzeau et al., 2010), SM Rac1 is not involved in the contraction or the relaxation of PASMCs, but that its role in PH is mediated by an increase in ROS production and proliferation of PASMCs.

Studies on the identification of the role of Rac1 in SMCs have produced conflicting results (Loirand & Pacaud, 2014). Indeed, in the vascular system, Rac1 is described to promote relaxation by regulating cGMP level in SMCs (Andre et al., 2014; Sauzeau et al., 2010) while it is involved in the contraction of visceral and bronchial SMCs (Andre-Gregoire et al., 2018; Rahman et al., 2014). These discrepancies suggest that the role of Rac1 depends on the type or tissue/organ location of SMCs and cannot be generalized to all SMCs. In the same line, we show in the present study that the role of Rac1 in PASMC is different from that in systemic arteries. In PA, SM Rac1 deletion has no direct effect on vasoconstriction or vasodilation. However, SM

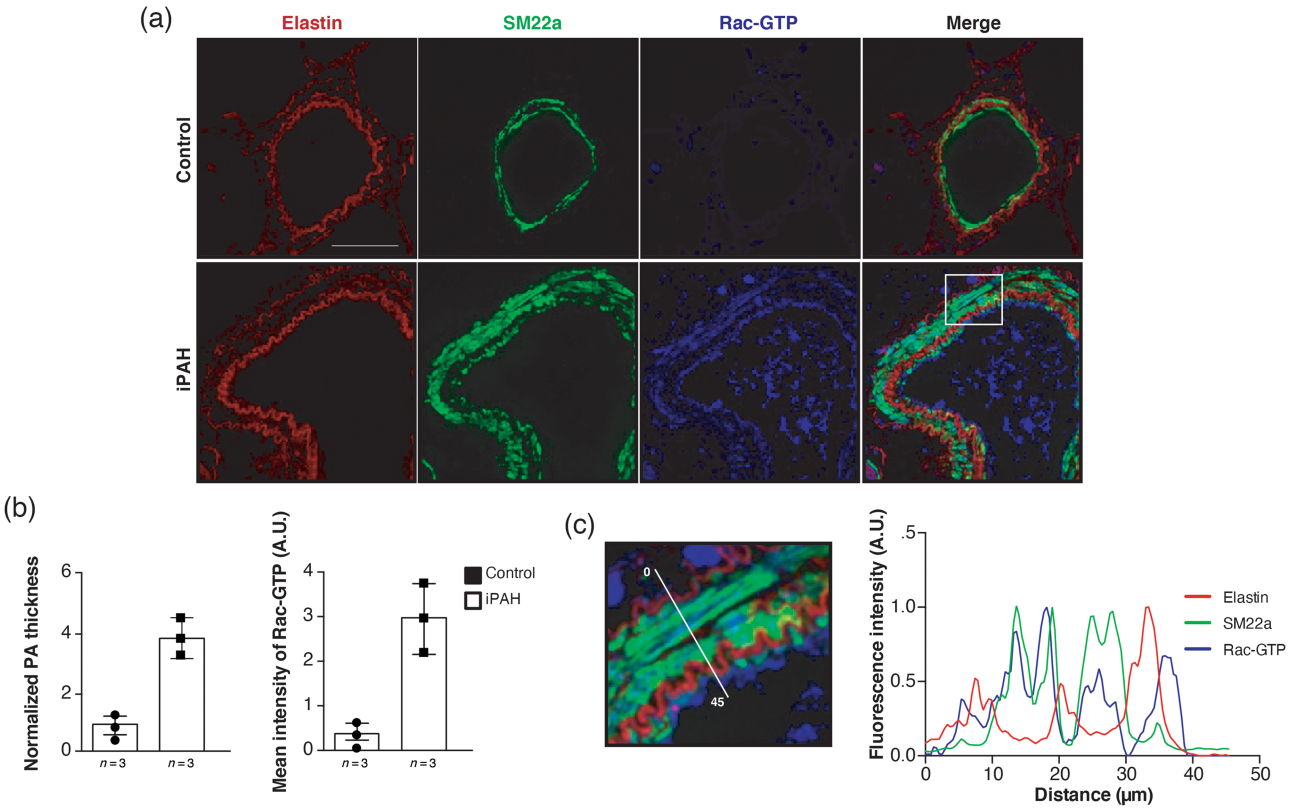

FIGURE 5 Rac1 is overactivated in pulmonary artery (PA) of idiopathic pulmonary arterial hypertension (iPAH) patients. (a) Representative confocal images of Rac-GTP immunofluorescence (blue) in cryosections of lung from control and iPAH patients. Arteries was detected by elastin autofluorescence (red), smooth muscle by SM22α immunofluorescence (green), and Rac1 activity by Rac-GTP immunofluorescence (blue). Scale bar = 80 µm. (b) Quantification of smooth muscle (SM) layer thickness and Rac1 activity (Rac-GTP labelling fluorescence intensity) in lung sections from control and iPAH patients. (c) Magnification corresponding to the white square in (a) and spatial profile of fluorescence intensity for indicated fluorescence channels for the white line positioned on the image. Data are expressed as mean ± SEM

Rac1 deletion improves endothelial-dependent PA vasodilation in mice exposed to chronic hypoxia, without having an effect on the dilation induced by a NO-donor (SNAP), suggesting a role of PASMC Rac1 upstream to the effect of endothelial NO on PASMC. Endothelial dysfunction in PA, characterized by impaired synthesis and/or bioactivity of endothelium-derived NO and a decrease in endothelium-dependent relaxation is recognized as a key event and a common feature of all types of PH, including hypoxic PH (Budhiraja et al., 2004; Hampl & Herget, 2000). This endothelial dysfunction has been ascribed, at least in part, to elevated level of NOX-derived ROS in experimental model of PH (Fresquet et al., 2006; Knock, 2019), in agreement with the increase in plasma oxidative stress biomarkers in PH patients (Reis et al., 2013). High levels of superoxide anion (O_2^-) favour its interaction with NO to produce peroxynitrite ($ONOO^-$), thus decreasing NO (Boota et al., 1996; Fresquet et al., 2006). Oxidative stress has become recognized as a central player in the underlying pathophysiology of PH and antioxidants or drugs that target specific sources of ROS, such as NOX, have been suggested as potential therapies for PH (Knock, 2019).

NOX1 and NOX2 are both expressed in PA, and NOX1- and NOX2-derived ROS have been shown to participate to PH in experimental animal models and in humans (Yan et al., 2020). NOX1 or NOX2 knockout in mice suppresses the increased right ventricular systolic pressure and prevents the right ventricular hypertrophy and vascular remodelling induced by chronic hypoxia (Hanna et al., 2004; Liu et al., 2006; Nisbet et al., 2009). Full activation of NOX1 or NOX2 allowing sustained long-lasting increase in ROS production is dependent on the recruitment of active Rac1 (or **Rac2**) that completes the assembly of the holoenzyme (Knock, 2019). Our results showing that chronic hypoxia-induced ROS production in the lungs is prevented in SM-Rac1-KO mice. This supports a major role of PASMC NOX1 and NOX2 in the generation of deleterious ROS in PH and demonstrate *in vivo* the essential role of Rac1 in the production of ROS by NOX1 and NOX2 without modification of their expression. They also prove the SMC origin of the ROS responsible for endothelial dysfunction, PASMCs proliferation and PA wall remodelling in hypoxic PH. As previously demonstrated *in vitro* (Diebold et al., 2008, 2010; Patil et al., 2004), Rac1-dependent ROS production in PASMCs is directly stimulated by hypoxia suggesting that chronic hypoxia in mice may be the trigger for Rac1 activation and Rac1-mediated stimulation of NOX involved *in vivo* in pulmonary vascular remodelling associated to hypoxic PH. However, besides hypoxia, vasoconstrictors and other receptor ligands such as 5-HT, ET-1 or EGF involved in PH and known to activate NOXs (Knock, 2019) are also described as Rac1 activators. This suggests that the involvement of Rac1 in NOX/ROS signalling in the pathogenesis of PH may not be limited to hypoxic PH but can be common to all types of PH. This is supported by the increase in Rac1 activity observed in PA of iPAH patients.

In conclusion, our study provides evidence that Rac1 activation in PASMC participates in the pathophysiology of PH by causing endothelial dysfunction and PASMC proliferation through increased production of ROS. In addition, it has been demonstrated that Rac1 in endothelial cells (Sun et al., 2020; Taraseviciene-Stewart et al., 2006; Yu et al., 2012), or in pulmonary artery fibroblasts (Zhang et al., 2020) plays a role in the development of pulmonary hypertension, supporting the idea that pharmacological inhibition of Rac1 may restrict disease progression and improve clinical outcomes of PH patients. To validate the therapeutic interest to inhibit Rac1 activity in PH, it will be necessary to develop specific and potent Rac1inhibitors suitable for *in vivo* analyses.

ACKNOWLEDGEMENTS

The authors thank Morgane Rousselle (l'institut du thorax) for expert technical assistance. We also value the support provided by the animal facility units of the University of Nantes. We thank Therassay, Micropicell and Cytocell core facilities (SFR François Bonamy, University of Nantes) for the functional and cellular explorations.

This work was supported by grants from the Institut de Recherche en Santé Respiratoire des Pays de la Loire (STARac and NARACAS projects) and the Institut National de la Santé et de la Recherche Médicale (INSERM). LR was supported by a grant from MRES. FD was supported by a grant from Fondation pour la Recherche Médicale.

AUTHOR CONTRIBUTIONS

C.G., G.L. and V.S. were responsible for the conception and design. F.D., M.R., L.R., A.T. and V.S. were responsible for the experimentation. G.L. and V.S. were responsible for the analysis and interpretation. F.D., G.L. and V.S. were responsible for drafting the manuscript.

CONFLICT OF INTEREST

The authors have reported that they have no relationships with industry relevant to the contents of this paper to disclose.

DECLARATION OF TRANSPARENCY AND SCIENTIFIC RIGOUR

This Declaration acknowledges that this paper adheres to the principles for transparent reporting and scientific rigour of preclinical research as stated in the *British Journal of Pharmacology* guidelines for Design and Analysis, Immunoblotting and Immunochemistry and Animal Experimentation, and as recommended by funding agencies, publishers and other organizations engaged with supporting research.

DATA AVAILABILITY STATEMENT

The data that support the findings of this study are available from the corresponding author upon reasonable request. Some data may not be made available because of privacy or ethical restrictions.

ORCID

Christophe Guignabert https://orcid.org/0000-0002-8545-4452
Vincent Sauzeau https://orcid.org/0000-0002-6187-0312

REFERENCES

Alexander, S. P., Christopoulos, A., Davenport, A. P., Kelly, E., Mathie, A., Peters, J. A., Veale, E. L., Armstrong, J. F., Faccenda, E., Harding, S. D., Pawson, A. J., Southan, C., Davies, J. A., Abbracchio, M. P., Alexander, W., Al-hosaini, K., Bäck, M., Barnes, N. M., Bathgate, R., …

Ye, R. D. (2021). The Concise Guide to PHARMACOLOGY 2021/22: G protein-coupled receptors. *British Journal of Pharmacology*, *178*(S1), S27–S156. https://doi.org/10.1111/bph.15538

Alexander, S. P., Fabbro, D., Kelly, E., Mathie, A., Peters, J. A., Veale, E. L., Armstrong, J. F., Faccenda, E., Harding, S. D., Pawson, A. J., Southan, C., Davies, J. A., Boison, D., Burns, K. E., Dessauer, C., Gertsch, J., Helsby, N. A., Izzo, A. A., Koesling, D., … Wong, S. S. (2021). The Concise Guide to PHARMACOLOGY 2021/22: Enzymes. *British Journal of Pharmacology*, *178*(S1), S313–S411. https://doi.org/10.1111/bph.15542

Alexander, S. P. H., Roberts, R. E., Broughton, B. R. S., Sobey, C. G., George, C. H., Stanford, S. C., Cirino, G., Docherty, J. R., Giembycz, M. A., Hoyer, D., Insel, P. A., Izzo, A. A., Ji, Y., MacEwan, D. J., Mangum, J., Wonnacott, S., & Ahluwalia, A. (2018). Goals and practicalities of immunoblotting and immunohistochemistry: A guide for submission to the British Journal of Pharmacology. *British Journal of Pharmacology*, *175*, 407–411. https://doi.org/10.1111/bph.14112

Andre, G., Sandoval, J. E., Retailleau, K., Loufrani, L., Toumaniantz, G., Offermanns, S., Rolli-Derkinderen, M., Loirand, G., & Sauzeau, V. (2014). Smooth muscle specific Rac1 deficiency induces hypertension by preventing p116RIP3-dependent RhoA inhibition. *Journal of the American Heart Association*, *3*, e000852.

Andre-Gregoire, G., Dilasser, F., Chesne, J., Braza, F., Magnan, A., Loirand, G., & Sauzeau, V. (2018). Targeting of Rac1 prevents bronchoconstriction and airway hyperresponsiveness. *The Journal of Allergy and Clinical Immunology*, *142*(824–833), e823.

Boota, A., Zar, H., Kim, Y. M., Johnson, B., Pitt, B., & Davies, P. (1996). IL-1 beta stimulates superoxide and delayed peroxynitrite production by pulmonary vascular smooth muscle cells. *The American Journal of Physiology*, *271*, L932–L938.

Budhiraja, R., Tuder, R. M., & Hassoun, P. M. (2004). Endothelial dysfunction in pulmonary hypertension. *Circulation*, *109*(2), 159–165. https://doi.org/10.1161/01.CIR.0000102381.57477.50

Curtis, M. J., Alexander, S., Cirino, G., Docherty, J. R., George, C. H., Giembycz, M. A., Hoyer, D., Insel, P. A., Izzo, A. A., Ji, Y., MacEwan, D. J., Sobey, C. G., Stanford, S. C., Teixeira, M. M., Wonnacott, S., & Ahluwalia, A. (2018). Experimental design and analysis and their reporting II: Updated and simplified guidance for authors and peer reviewers. *British Journal of Pharmacology*, *175*(7), 987–993. https://doi.org/10.1111/bph.14153

Diebold, I., Djordjevic, T., Hess, J., & Gorlach, A. (2008). Rac-1 promotes pulmonary artery smooth muscle cell proliferation by upregulation of plasminogen activator inhibitor-1: Role of NFkappaB-dependent hypoxia-inducible factor-1alpha transcription. *Thrombosis and Haemostasis*, *100*, 1021–1028. https://doi.org/10.1160/TH08-07-0473

Diebold, I., Petry, A., Djordjevic, T., Belaiba, R. S., Fineman, J., Black, S., Schreiber, C., Fratz, S., Hess, J., Kietzmann, T., & Görlach, A. (2010). Reciprocal regulation of Rac1 and PAK-1 by HIF-1alpha: A positive-feedback loop promoting pulmonary vascular remodeling. *Antioxidants & Redox Signaling*, *13*, 399–412. https://doi.org/10.1089/ars.2009.3013

Dumas de la Roque, E., Smeralda, G., Quignard, J. F., Freund-Michel, V., Courtois, A., Marthan, R., Muller, B., Guibert, C., & Dubois, M. (2017). Altered vasoreactivity in neonatal rats with pulmonary hypertension associated with bronchopulmonary dysplasia: Implication of both eNOS phosphorylation and calcium signaling. *PLoS ONE*, *12*, e0173044. https://doi.org/10.1371/journal.pone.0173044

Fresquet, F., Pourageaud, F., Leblais, V., Brandes, R. P., Savineau, J. P., Marthan, R., & Muller, B. (2006). Role of reactive oxygen species and gp91phox in endothelial dysfunction of pulmonary arteries induced by chronic hypoxia. *British Journal of Pharmacology*, *148*, 714–723. https://doi.org/10.1038/sj.bjp.0706779

Galiè, N., Brundage, B. H., Ghofrani, H. A., Oudiz, R. J., Simonneau, G., Safdar, Z., Shapiro, S., White, R. J., Chan, M., Beardsworth, A., Frumkin, L., & Barst, R. J. (2009). Tadalafil therapy for pulmonary arterial hypertension. *Circulation*, *119*, 2894–2903. https://doi.org/10.1161/CIRCULATIONAHA.108.839274

Galiè, N., Rubin, L., Hoeper, M., Jansa, P., al-Hiti, H., Meyer, G., Chiossi, E., Kusic-Pajic, A., & Simonneau, G. (2008). Treatment of patients with mildly symptomatic pulmonary arterial hypertension with bosentan (EARLY study): A double-blind, randomised controlled trial. *Lancet*, *371*, 2093–2100. https://doi.org/10.1016/S0140-6736(08)60919-8

Hampl, V., & Herget, J. (2000). Role of nitric oxide in the pathogenesis of chronic pulmonary hypertension. *Physiological Reviews*, *80*(4), 1337–1372. https://doi.org/10.1152/physrev.2000.80.4.1337

Hanna, I. R., Hilenski, L. L., Dikalova, A., Taniyama, Y., Dikalov, S., Lyle, A., Quinn, M. T., Lassègue, B., & Griendling, K. K. (2004). Functional association of nox1 with p22phox in vascular smooth muscle cells. *Free Radical Biology & Medicine*, *37*, 1542–1549. https://doi.org/10.1016/j.freeradbiomed.2004.08.011

Hordijk, P. L. (2006). Regulation of NADPH oxidases: The role of Rac proteins. *Circulation Research*, *98*, 453–462. https://doi.org/10.1161/01.RES.0000204727.46710.5e

Humbert, M., Guignabert, C., Bonnet, S., Dorfmüller, P., Klinger, J. R., Nicolls, M. R., Olschewski, A. J., Pullamsetti, S. S., Schermuly, R. T., Stenmark, K. R., & Rabinovitch, M. (2019). Pathology and pathobiology of pulmonary hypertension: State of the art and research perspectives. *The European Respiratory Journal*, *53*, 1801887. https://doi.org/10.1183/13993003.01887-2018

Humbert, M., Morrell, N. W., Archer, S. L., Stenmark, K. R., MacLean, M. R., Lang, I. M., Christman, B. W., Weir, E. K., Eickelberg, O., Voelkel, N. F., & Rabinovitch, M. (2004). Cellular and molecular pathobiology of pulmonary arterial hypertension. *Journal of the American College of Cardiology*, *43*, S13–S24. https://doi.org/10.1016/j.jacc.2004.02.029

Izzo, A. A., Teixeira, M., Alexander, S. P., Cirino, G., Docherty, J. R., George, C. H., Insel, P. A., Ji, Y., Kendall, D. A., Panattieri, R. A., Sobey, C. G., Stanford, S. C., Stefanska, B., Stephens, G., & Ahluwalia, A. (2020). A practical guide for transparent reporting of research on natural products in the *British Journal of Pharmacology*: Reproducibility of natural product research. *British Journal of Pharmacology*, *177*(10), 2169–2178. https://doi.org/10.1111/bph.15054

Knock, G. A. (2019). NADPH oxidase in the vasculature: Expression, regulation and signalling pathways; role in normal cardiovascular physiology and its dysregulation in hypertension. *Free Radical Biology & Medicine*, *145*, 385–427. https://doi.org/10.1016/j.freeradbiomed.2019.09.029

Li, Q., Qiu, Y., Mao, M., Lv, J., Zhang, L., Li, S., Li, X., & Zheng, X. (2014). Antioxidant mechanism of Rutin on hypoxia-induced pulmonary arterial cell proliferation. *Molecules*, *19*, 19036–19049. https://doi.org/10.3390/molecules191119036

Lilley, E., Stanford, S. C., Kendall, D. E., Alexander, S. P., Cirino, G., Docherty, J. R., George, C. H., Insel, P. A., Izzo, A. A., Ji, Y., Panettieri, R. A., Sobey, C. G., Stefanska, B., Stephens, G., Teixeira, M., & Ahluwalia, A. (2020). ARRIVE 2.0 and the *British Journal of Pharmacology*: Updated guidance for 2020. *British Journal of Pharmacology*, *177*(16), 3611–3616. https://doi.org/10.1111/bph.15178

Liu, J. Q., Zelko, I. N., Erbynn, E. M., Sham, J. S., & Folz, R. J. (2006). Hypoxic pulmonary hypertension: Role of superoxide and NADPH oxidase (gp91phox). *American Journal of Physiology. Lung Cellular and Molecular Physiology*, *290*, L2–L10. https://doi.org/10.1152/ajplung.00135.2005

Loirand, G., & Pacaud, P. (2014). Involvement of Rho GTPases and their regulators in the pathogenesis of hypertension. *Small GTPases*, *5*, 1–10. https://doi.org/10.4161/sgtp.28846

Loirand, G., Sauzeau, V., & Pacaud, P. (2013). Small G proteins in the cardiovascular system: Physiological and pathological aspects. *Physiological Reviews*, *93*, 1659–1720. https://doi.org/10.1152/physrev.00021.2012

Lyle, M. A., Davis, J. P., & Brozovich, F. V. (2017). Regulation of pulmonary vascular smooth muscle contractility in pulmonary arterial hypertension: Implications for therapy. *Frontiers in Physiology*, *8*, 614. https://doi.org/10.3389/fphys.2017.00614

McLaughlin, V. V., Shah, S. J., Souza, R., & Humbert, M. (2015). Management of pulmonary arterial hypertension. *Journal of the American College of Cardiology*, *65*, 1976–1997. https://doi.org/10.1016/j.jacc.2015.03.540

McLaughlin, V. V., Shillington, A., & Rich, S. (2002). Survival in primary pulmonary hypertension: The impact of epoprostenol therapy. *Circulation*, *106*, 1477–1482. https://doi.org/10.1161/01.CIR.0000029100.82385.58

Nisbet, R. E., Graves, A. S., Kleinhenz, D. J., Rupnow, H. L., Reed, A. L., Fan, T. H., Mitchell, P. O., Sutliff, R. L., & Hart, C. M. (2009). The role of NADPH oxidase in chronic intermittent hypoxia-induced pulmonary hypertension in mice. *American Journal of Respiratory Cell and Molecular Biology*, *40*, 601–609. https://doi.org/10.1165/2008-0145OC

Patil, S., Bunderson, M., Wilham, J., & Black, S. M. (2004). Important role for Rac1 in regulating reactive oxygen species generation and pulmonary arterial smooth muscle cell growth. *American Journal of Physiology. Lung Cellular and Molecular Physiology*, *287*, L1314–L1322. https://doi.org/10.1152/ajplung.00383.2003

Percie du Sert, N., Hurst, V., Ahluwalia, A., Alam, S., Avey, M. T., Baker, M., Browne, W. J., Clark, A., Cuthill, I. C., Dirnagl, U., Emerson, M., Garner, P., Holgate, S. T., Howells, D. W., Karp, N. A., Lazic, S. E., Lidster, K., MacCallum, C. J., Macleod, M., … Würbel, H. (2020). The ARRIVE guidelines 2.0: updated guidelines for reporting animal research. *PLoS Biology*, *18*(7), e3000410. https://doi.org/10.1371/journal.pbio.3000410

Rahman, A., Davis, B., Lövdahl, C., Hanumaiah, V. T., Feil, R., Brakebusch, C., & Arner, A. (2014). The small GTPase Rac1 is required for smooth muscle contraction. *The Journal of Physiology*, *592*, 915–926. https://doi.org/10.1113/jphysiol.2013.262998

Reis, G. S., Augusto, V. S., Silveira, A. P., Jordão, A. A. Jr., Baddini-Martinez, J., Neto, O. P., Rodrigues, A. J., & Evora, P. R. B. (2013). Oxidative-stress biomarkers in patients with pulmonary hypertension. *Pulmonary Circulation*, *3*, 856–861. https://doi.org/10.1086/674764

Sauzeau, V., Sevilla, M. A., Montero, M. J., & Bustelo, X. R. (2010). The Rho/Rac exchange factor Vav2 controls nitric oxide-dependent responses in mouse vascular smooth muscle cells. *The Journal of Clinical Investigation*, *120*, 315–330. https://doi.org/10.1172/JCI38356

Simonneau, G., Montani, D., Celermajer, D. S., Denton, C. P., Gatzoulis, M. A., Krowka, M., Williams, P. G., & Souza, R. (2019). Haemodynamic definitions and updated clinical classification of pulmonary hypertension. *The European Respiratory Journal*, *53*, 1801913. https://doi.org/10.1183/13993003.01913-2018

Sitbon, O., Gomberg-Maitland, M., Granton, J., Lewis, M. I., Mathai, S. C., Rainisio, M., Stockbridge, N. L., Wilkins, M. R., Zamanian, R. T., & Rubin, L. J. (2019). Clinical trial design and new therapies for pulmonary arterial hypertension. *The European Respiratory Journal*, *53*, 1801908. https://doi.org/10.1183/13993003.01908-2018

Sitbon, O., Humbert, M., & Simonneau, G. (2002). Primary pulmonary hypertension: Current therapy. *Progress in Cardiovascular Diseases*, *45*, 115–128. https://doi.org/10.1053/pcad.2002.128449

Sun, X., Lu, Q., Yegambaram, M., Kumar, S., Qu, N., Srivastava, A., Wang, T., Fineman, J. R., & Black, S. M. (2020). TGF-beta1 attenuates mitochondrial bioenergetics in pulmonary arterial endothelial cells via the disruption of carnitine homeostasis. *Redox Biology*, *36*, 101593. https://doi.org/10.1016/j.redox.2020.101593

Taraseviciene-Stewart, L., Scerbavicius, R., Choe, K. H., Cool, C., Wood, K., Tuder, R. M., Burns, N., Kasper, M., & Voelkel, N. F. (2006). Simvastatin causes endothelial cell apoptosis and attenuates severe pulmonary hypertension. *American Journal of Physiology. Lung Cellular and Molecular Physiology*, *291*, L668–L676. https://doi.org/10.1152/ajplung.00491.2005

Tesse, A., Gena, P., Rützler, M., & Calamita, G. (2021). Ablation of aquaporin-9 ameliorates the systemic inflammatory response of LPS-induced endotoxic shock in mouse. *Cell*, *10*(2), 435. https://doi.org/10.3390/cells10020435

Thenappan, T., Ormiston, M. L., Ryan, J. J., & Archer, S. L. (2018). Pulmonary arterial hypertension: Pathogenesis and clinical management. *BMJ*, *360*, j5492.

Wang, X., & Sun, Z. (2010). Thyroid hormone induces artery smooth muscle cell proliferation: Discovery of a new TRalpha1-Nox1 pathway. *Journal of Cellular and Molecular Medicine*, *14*, 368–380. https://doi.org/10.1111/j.1582-4934.2008.00489.x

Wang, Y., Ji, L., Jiang, R., Zheng, L., & Liu, D. (2014). Oxidized high-density lipoprotein induces the proliferation and migration of vascular smooth muscle cells by promoting the production of ROS. *Journal of Atherosclerosis and Thrombosis*, *21*, 204–216. https://doi.org/10.5551/jat.19448

Watanabe, H. (2018). Treatment selection in pulmonary arterial hypertension: Phosphodiesterase type 5 inhibitors versus soluble guanylate cyclase stimulator. *European Cardiology*, *13*, 35–37. https://doi.org/10.15420/ecr.2017:22:2

Yan, S., Resta, T. C., & Jernigan, N. L. (2020). Vasoconstrictor mechanisms in chronic hypoxia-induced pulmonary hypertension: Role of oxidant signaling. *Antioxidants (Basel, Switzerland)*, *9*(10), 999. https://doi.org/10.3390/antiox9100999

Yu, M., Gong, D., Lim, M., Arutyunyan, A., Groffen, J., & Heisterkamp, N. (2012). Lack of bcr and abr promotes hypoxia-induced pulmonary hypertension in mice. *PLoS ONE*, *7*, e49756. https://doi.org/10.1371/journal.pone.0049756

Zhang, S., Yin, Z., Qin, W., Ma, X., Zhang, Y., Liu, E., & Chu, Y. (2020). Pirfenidone inhibits hypoxic pulmonary hypertension through the NADPH/ROS/p38 pathway in adventitial fibroblasts in the pulmonary artery. *Mediators of Inflammation*, *2020*, 2604967.

How to cite this article: Dilasser, F., Rio, M., Rose, L., Tesse, A., Guignabert, C., Loirand, G., & Sauzeau, V. (2022). Smooth muscle Rac1 contributes to pulmonary hypertension. *British Journal of Pharmacology*, *179*(13), 3418–3429. https://doi.org/10.1111/bph.15805